Zhou and Wu *Boundary Value Problems* (2016) 2016:48
DOI 10.1186/s13661-016-0546-2

Boundary Value Problems
a SpringerOpen Journal

RESEARCH Open Access

Simulation of blow-up solutions to the generalized KdV equations by moving collocation methods

Zhiqiang Zhou* and Xiaodan Wu

*Correspondence:
zqzhou@2014.swufe.edu.cn
School of Economic Mathematics, Southwestern University of Finance and Economics, Chengdu, Wenjiang 611130, P.R. China

Abstract

The aim of this paper is to simulate the blow-up solutions to generalized Korteweg-de Vries (KdV) equations. The KdV equations are discretized with the use of a quintic Hermite collocation method based on the moving meshes generated by solving moving mesh partial differential equations (MMPDEs). Theoretical analyses are, respectively, conducted to determine the critical parameters in MMPDEs such that the generated meshes can catch up with the blow-up profiles and to show the effectiveness of the generated moving meshes. Lastly, a variety of examples are implemented to confirm our analysis and show the efficiency of the method.

MSC: 35Q51; 35Q53; 65N50; 65N35

Keywords: Korteweg-de Vries equations; moving mesh methods; dimensional analysis; blow-up solution

1 Introduction

The focus of this paper is on numerical simulations of blow-up solutions to the generalized Korteweg-de Vries (GKdV) equation

$$u_t + u^p u_x + \epsilon u_{xxx} = 0, \quad x \in (a, b), \tag{1}$$

with periodic boundary conditions, where ϵ is a positive number and p a positive integer.

The special case $p = 1$ is the standard KdV equation (*e.g.*, [1]), and $p = 2$ corresponds to the modified KdV equation (*e.g.*, [2]). The theoretical analysis by Bona *et al.* [3] shows that the solitary-wave solutions are stable if and only if $p < 4$. Bona *et al.* [4] also show that the solutions for $p \geq 4$ exhibit finite blow-up phenomena with a similarity form

$$u(x,t) = (T-t)^{-2/(3p)} \psi\left(\frac{x^* - x - c(T-t)^{1/3}}{(T-t)^{1/3}}\right) + \text{bounded term}, \tag{2}$$

where x^*, T, c are real parameters and the similarity profile ψ is a smooth function which tends to zero at $\pm\infty$. The point at which the peak value occurs depends on time in the form $x(t) = x^* + c(T-t)^{1/3}$, and, obviously, $x \to x^*$ as $t \to T$.

To compute such a type of singularities sufficiently and effectively, and hence to mimic the asymptotic behavior of the solution as $t \to T$, the numerical method employed is required to adapt the spatial meshes to the evolving singularities. In order to achieve this, Bona *et al.* employ the h-adaptation technique [5, 6]: a spatial translation is used to keep the blow-up peak appearing near the fixed point $x = 0.5$ and local mesh refinement is conducted recursively right around this point. The demerit of this local refinement technique is that the computational cost becomes larger and larger as the blow-up solution evolves. Moreover, the use of interpolations in the time integration does not keep the truncation errors under control. In this paper, based on the moving mesh method, we provide a more reliable simulation method along with an in-depth analysis.

Let a coordinate be

$$\mu = \left[x - x^* - c(T-t)^{1/3}\right](T-t)^{-1/3}. \tag{3}$$

Then the blow-up profile can be represented by this coordinate. The mesh movement is based on the time-dependent mapping

$$x(\cdot, t) : I_c \to I = [x_L, x_R],$$

where x_L, x_R are the left and right boundary points for the physical equation, and I_c is a computational space in which uniform grids will be taken. When I_c is taken as $[0,1]$ for example, the moving mesh can be generated by $x_j(j/N, t), j = 0, 1, \ldots, N$. The function $u(x,t)$ in physical variables can be transformed into the function in computational variables

$$u(x,t) = u\big(x(\xi,t),t\big),$$

and the blow-up profile is expressed in the computational variable ξ. Equation (3) suggests that in order to keep up with the blow-up profiles, the mesh trajectory speed has to satisfy

$$[\dot{x}] = \frac{[x]}{[t]} \geq [t]^{-2/3}, \tag{4}$$

whereafter we use $[u]$, $[t]$, and $[x]$ to denote the dimensions of the variables u, t, and x, respectively. For the underlying physical PDEs (1) the time scale should be taken as $[t] = T - t$. Dimensional analysis, more often used by physicians, is a tool to find or check relations among physical quantities. In our paper, we use this technique to approximately determine the relations among some dominant quantities in the equation with blow-up solutions, and this method was first used by Budd *et al.* in [7].

The moving mesh function $x(\xi, t)$ satisfies certain parabolic equations which are called moving mesh partial differential equations (MMPDEs). Two MMPDEs (MMPDE5, MMPDE6) in [8] are considered in this paper, namely,

$$\dot{x} = \frac{1}{\tau}\frac{\partial}{\partial \xi}\left(M\frac{\partial x}{\partial \xi}\right), \tag{5}$$

$$-\frac{\partial^2 \dot{x}}{\partial \xi^2} = \frac{1}{\tau}\frac{\partial}{\partial \xi}\left(M\frac{\partial x}{\partial \xi}\right), \tag{6}$$

with

$$x(0,t) = a, \qquad x(1,t) = b. \tag{7}$$

Here $M = M(x,t)$ is the monitor function which depends on the physical solution and is used for controlling mesh concentration, while $\tau = \tau(t) > 0$ is a parameter used for adjusting the response time of mesh movement to changes in M. The two MMPDEs are obtained based on attraction and repulsion pseudoforces between nodes. They are also related to the equidistribution equation,

$$0 = \frac{\partial}{\partial \xi}\left(M\frac{\partial x}{\partial \xi}\right). \tag{8}$$

It can be observed that, for both MMPDE5 and MMPDE6, the mesh trajectory speeds depend on M and τ. Moreover, for any choice of M and τ, the two MMPDEs can generate smooth meshes as long as the time scale is taken to be sufficiently small. Therefore, the key issues we need to deal with in the simulation of blow-up are: 1. how to choose M and τ so that the mesh trajectory speed is as fast as that in (4); 2. how small the time scale should be in order that the MMPDEs can generate smooth meshes and resolve the dramatically increase in the blow-up solution.

The dimensional equation for both MMPDE5 and MMPDE6 is

$$[\dot{x}] = \frac{[M][x]}{[\tau]}.$$

In view of (4), to capture the blow-up profiles, it is required that

$$\frac{[M][x]}{[\tau]} \geq [t]^{-2/3}. \tag{9}$$

Based on the moving mesh $x(\xi,t)$, a conservative moving collocation method with quintic Hermite spline basis is employed to discretize the GKdV equation (1). The conservative moving collocation method with cubic Hermite spline basis was proposed by Huang and Russell in [9] to solve second-order time-dependent PDEs. Later moving collocation methods were developed to solve fourth-order PDEs [10] and fractional-order PDEs [11]. The convergence analysis of the moving collocation methods was given by Ma *et al.* [12].

Among the earlier literature which uses MMPDE5 and MMPDE6 to generate moving meshes in the simulation of blow-up solutions, Huang *et al.* [13] chose the monitor parameters M and τ according to what is called 'the dominance of equidistribution', and introduced dimensional analysis. Different from [13], our paper uses the criterion that the mesh trajectory speed satisfies (4) for determining the parameters M and τ, as stated above, and presents a theoretical analysis to show the efficiency of the generated meshes.

We organize the paper as follows: in Section 2, the conservative moving collocation method of the fifth order is proposed to discretize (1); in Section 3, through dimensional analysis, we discuss the choices of the monitor function M and the parameter τ in the MMPDEs; in Section 4, the efficiency of the moving mesh collocation is analyzed; in Section 5, numerical examples are carried out to confirm our analysis and to simulate the blow-up.

2 The conservative moving collocation method

The conservative moving collocation method, which is introduced by Huang and Russell [14], will be used to discretize the main equation. To this end, we reformulate the GKdV equation (1) into the following form:

$$F(u_t) = \big[G(u, u_{xx})\big]_x, \tag{10}$$

where $F(u_t) = u_t$ and $G(u, u_{xx}) = -\frac{1}{p+1}u^{p+1} - u_{xx}$. Define a time mesh

$$0 = t_0 < t_1 < \cdots < t_L.$$

Denote the time-dependent spatial mesh at time t_n $(n = 0, 1, \ldots)$ by

$$a = x_0^n < x_1^n < \cdots < x_N^n = b.$$

Denote the size of the jth interval by $h_j^n = x_j^n - x_{j-1}^n$, $j = 1, 2, \ldots, N$. Divide each interval equally into three parts by inserting two points $x_{j+\frac{k}{3}}^n = x_j^n + \frac{k}{3}h_{j+1}^n$, $k = 1, 2$. Integrating (10) over $I_{j,k}^n = [x_{j+\frac{k}{3}}^n, x_{j+\frac{k+1}{3}}^n]$, $k = 0, 1, 2$, gives

$$\int_{I_{j,k}^n} F(u_t)dx = G(u, u_{xx})|_{x=x_{j+\frac{k+1}{3}}^n} - G(u, u_{xx})|_{x=x_{j+\frac{k}{3}}^n}. \tag{11}$$

On intervals $[x_j^n, x_{j+1}^n]$ $(j = 0, 1, \ldots, N-1)$, $u(x, t_n)$ is approximated by a fifth-order Hermite polynomial

$$\begin{aligned} v^n(x) = {} & v_j^n\phi_1(s) + v_{x,j}^n h_{j+1}^n\phi_2(s) + v_{xx,j}^n\big(h_{j+1}^n\big)^2\phi_3(s) \\ & + v_{j+1}^n\phi_4(s) + v_{x,j+1}^n h_{j+1}^n\phi_5(s) + v_{xx,j+1}^n\big(h_{j+1}^n\big)^2\phi_6(s), \end{aligned}$$

where v_j^n, $v_{x,j}^n$, $v_{xx,j}^n$ denote the approximations to $u(x_j^n, t_n)$, $u_x(x_j^n, t_n)$, $u_{xx}(x_j^n, t_n)$, respectively. The local coordinate s is defined by

$$s = \frac{x - x_j^n}{h_{j+1}^n},$$

and the Hermite basis functions are given by

$$\begin{aligned} &\phi_1(s) = \big(-6s^2 - 3s - 1\big)(s-1)^3, \quad \phi_2(s) = -s(3s+1)(s-1)^3, \quad \phi_3(s) = -1/2s^2(s-1)^3, \\ &\phi_4(s) = \big(6s^2 - 15s + 10\big)s^3, \quad \phi_5(s) = -(s-1)(3s-4)s^3, \quad \phi_6(s) = 1/2(s-1)^2s^3. \end{aligned}$$

In order to obtain an algorithm which is second order in time, we consider the approximation to $u(x, t_{n-1/2})$, where $t_{n-1/2} \equiv \frac{t_{n-1}+t_n}{2}$, defined by

$$\begin{aligned} v^{n-1/2}(x) = {} & \frac{\tilde{v}_j^{n-1} + v_j^n}{2}\phi_1(s) + \frac{\tilde{v}_{x,j}^{n-1} + v_{x,j}^n}{2}h_{j+1}^n\phi_2(s) + \frac{\tilde{v}_{xx,j}^{n-1} + v_{xx,j}^n}{2}\big(h_{j+1}^n\big)^2\phi_3(s) \\ & + \frac{\tilde{v}_{j+1}^{n-1} + v_{j+1}^n}{2}\phi_4(s) + \frac{\tilde{v}_{x,j+1}^{n-1} + v_{x,j+1}^n}{2}h_{j+1}^n\phi_5(s) + \frac{\tilde{v}_{xx,j+1}^{n-1} + v_{xx,j+1}^n}{2}\big(h_{j+1}^n\big)^2\phi_6(s), \end{aligned}$$

for $x \in [x_j^n, x_{j+1}^n]$, $j = 0, 1, \ldots, N-1$, $u(x, t_{n-1/2})$, where

$$\tilde{v}_j^{n-1} = v^{n-1}\big(x_j^n\big), \qquad \tilde{v}_{x,j}^{n-1} = v_x^{n-1}\big(x_j^n\big), \qquad \tilde{v}_{xx,j}^{n-1} = v_{xx}^{n-1}\big(x_j^n\big).$$

Similarly, we define the approximations to $u_x(x, t_{n-1/2})$ and $u_{xx}(x, t_{n-1/2})$, respectively, by

$$\begin{aligned} v_x^{n-1/2}(x) = \frac{1}{h_{j+1}^n}\Bigg[& \frac{\tilde{v}_j^{n-1} + v_j^n}{2}\phi_1(s) + \frac{\tilde{v}_{x,j}^{n-1} + v_{x,j}^n}{2}h_{j+1}^n\phi_2(s) + \frac{\tilde{v}_{xx,j}^{n-1} + v_{xx,j}^n}{2}\big(h_{j+1}^n\big)^2\phi_3(s) \\ & + \frac{\tilde{v}_{j+1}^{n-1} + v_{j+1}^n}{2}\phi_4(s) + \frac{\tilde{v}_{x,j+1}^{n-1} + v_{x,j+1}^n}{2}h_{j+1}^n\phi_5(s) + \frac{\tilde{v}_{xx,j+1}^{n-1} + v_{xx,j+1}^n}{2}\big(h_{j+1}^n\big)^2\phi_6(s)\Bigg] \end{aligned}$$

and

$$\begin{aligned} v_{xx}^{n-1/2}(x) = \frac{1}{(h_{j+1}^n)^2}\Bigg[& \frac{\tilde{v}_j^{n-1} + v_j^n}{2}\phi_1(s) + \frac{\tilde{v}_{x,j}^{n-1} + v_{x,j}^n}{2}h_{j+1}^n\phi_2(s) + \frac{\tilde{v}_{xx,j}^{n-1} + v_{xx,j}^n}{2}\big(h_{j+1}^n\big)^2\phi_3(s) \\ & + \frac{\tilde{v}_{j+1}^{n-1} + v_{j+1}^n}{2}\phi_4(s) + \frac{\tilde{v}_{x,j+1}^{n-1} + v_{x,j+1}^n}{2}h_{j+1}^n\phi_5(s) + \frac{\tilde{v}_{xx,j+1}^{n-1} + v_{xx,j+1}^n}{2}\big(h_{j+1}^n\big)^2\phi_6(s)\Bigg]. \end{aligned}$$

Lastly, we define the approximation to $u_t(x, t_{n-1/2})$ as

$$\begin{aligned} v_t^{n-1/2}(x) = & \frac{v_j^n - \tilde{v}_j^{n-1}}{\Delta t_n}\phi_1(s) + \frac{v_{x,j}^n - \tilde{v}_{x,j}^{n-1}}{\Delta t_n}h_{j+1}^n\phi_2(s) + \frac{v_{xx,j}^n - \tilde{v}_{xx,j}^{n-1}}{\Delta t_n}\big(h_{j+1}^n\big)^2\phi_3(s) \\ & + \frac{v_j^n - \tilde{v}_j^{n-1}}{\Delta t_n}\phi_4(s) + \frac{v_{x,j}^n - \tilde{v}_{x,j}^{n-1}}{\Delta t_n}h_{j+1}^n\phi_5(s) + \frac{v_{xx,j+1}^n - \tilde{v}_{xx,j+1}^{n-1}}{\Delta t_n}\big(h_{j+1}^n\big)^2\phi_6(s), \end{aligned}$$

where $\Delta t_n = t_n - t_{n-1}$.

Substituting the above defined approximations into (11) gives, for $k = 0, 1, 2$; $j = 0, \ldots, N-1$,

$$\int_{I_{j,k}^n} F\big(v_t^{n-1/2}(x)\big)dx = G\big(v^{n-1/2}, v_{xx}^{n-1/2}\big)\big|_{x=x_{j+\frac{k+1}{3}}^n} - G\big(v^{n-1/2}, v_{xx}^{n-1/2}\big)\big|_{x=x_{j+\frac{k}{3}}^n}, \tag{12}$$

subject to periodic boundary conditions

$$v_0^n = v_N^n, \qquad v_{x,0}^n = v_{x,N}^n, \qquad v_{xx,0}^n = v_{xx,N}^n. \tag{13}$$

{(12), (13)} is the discretization of the original problem (1). The integral on the left-hand side of (12) is computed by the two-point Gauss quadrature formula.

3 Choice of monitor functions

We will consider three types of monitor functions in the MMPDEs for generating the moving mesh, namely

$$M = |u|^{\gamma_1}, \tag{14}$$

$$M = \left|\frac{\partial u}{\partial x}\right|^{\gamma_2}, \tag{15}$$

$$M = \alpha|u|^{\gamma_1} + (1-\alpha)\left|\frac{\partial u}{\partial x}\right|^{\gamma_2} \quad \text{with } 0 < \alpha < 1. \tag{16}$$

Our numerical results show that the first type (polynomial type) of monitor function is capable of simulating the blow-up phenomena, but it fails to capture the solitary waves. Therefore, the second monitor function based on gradient will be used on the purpose of capturing the blow-up and solitary waves later on. The third monitor function is the average of the first two, in which the parameter $0 < \alpha < 1$ is used to control the percentage of the mesh points being distributed to the solitary wave region and the blow-up region. In the following, we determine the parameters γ_1, γ_2, and τ using dimensional analysis introduced in [13] such that mesh trajectory speeds satisfy (4).

We begin with the physical equation (1). The dimensions of the terms u_t, $u^p u_x$, and u_{xxx} are

$$[u_t] = \frac{[u]}{[t]}, \qquad \left[u^p u_x\right] = \frac{[u]^{p+1}}{[x]}, \qquad [u_{xxx}] = \frac{[u]}{[x]^3}.$$

The dimensional balance for the physical PDE implies

$$\frac{[u]}{[t]} = \frac{[u]^{p+1}}{[x]} = \frac{[u]}{[x]^3}.$$

This yields the dimension relations

$$[x] = [t]^{1/3}, \qquad [u] = [t]^{-2/(3p)}. \tag{17}$$

So if the dimension of t is changed by a factor of $\lambda > 0$, the dimensions of x and u must vary by factors of $\lambda^{1/3}$ and $\lambda^{-2/(3p)}$, respectively, to keep the physical equation dimensionally balanced. This suggests a scaling transform

$$t \to \lambda t, \qquad x \to \lambda^{1/3} x, \qquad u \to \lambda^{-2/(3p)} u, \tag{18}$$

which can easily be proved to make the physical equation invariant. In fact, Bona *et al.* [4] used the same scaling transformation to obtain the similarity form of the blow-up solution (2).

Monitor function $M = |u|^{\gamma_1}$: The dimension analysis for MMPDE5 or MMPDE6 gives

$$[\dot{x}] = \frac{[x]}{[t]} = \frac{[u]^{\gamma_1}[x]}{[\tau]} = \frac{1}{[\tau][t]^{2\gamma_1/(3p)-1/3}}. \tag{19}$$

In the following, we discuss the case with a constant τ and that with a varying τ separately.

Constant τ: For the situation of constant τ, *i.e.*, τ is dimensionless, to make the mesh trajectory speed reach

$$[\dot{x}] \geq [t]^{-2/3}, \tag{20}$$

it requires

$$\frac{2\gamma_1}{3p} - \frac{1}{3} \geq \frac{2}{3} \quad \text{or} \quad \gamma_1 \geq \frac{3p}{2}. \tag{21}$$

For the critical case with

$$\gamma_1 = \frac{3p}{2}, \tag{22}$$

the constant τ should be sufficiently small to ensure a fast enough mesh trajectory speed. It should also be noted that the smaller the value of τ is taken, the faster is the mesh speed. Therefore, our goal is to choose a suitable value of τ such that the mesh moves fast enough to keep up with the moving blow-up profile while not too fast in order to guarantee the generation of smooth meshes.

Moreover, notice that blow-up only occurs in the solution to GKdV equations with $p > 4$. Even if we can obtain a satisfactory mesh trajectory speed by choosing a monitor function as $|u|^{\gamma_1}$ with $\gamma_1 \geq \frac{3p}{2}$, such a large power of the solution will generally result in over-concentration of the mesh points within the blow-up region and cause the simulation to break down. The same problem also occurs when the monitor function is chosen to be (15) or (16). In view of this, we shall only consider the case that γ_1 and γ_2 have small values. In particular, we fix $\gamma_1 = \gamma_2 = 1$ while we vary the value of τ to obtain a satisfactory mesh speed in the rest of the paper.

Varying τ: That (20) holds requires the dimension relation

$$[\tau] \leq [t]^{1-2\gamma_1/(3p)} = [u]^{\gamma_1 - 3p/2}.$$

This suggests us to choose τ as

$$\tau(t) = \kappa \Big[\max_x \big| u(x,t) \big| \Big]^{\gamma_1 - 3p/2 - \varepsilon}, \tag{23}$$

where ε is some positive constant, and $\kappa > 0$ is a dimensionless constant which should be taken sufficient small for (23). With this choice of τ, the mesh trajectory speed will be fast enough so that the moving meshes generated by MMPDE5 or MMPDE6 can timely capture the blow-up profiles.

Monitor function $M = |\frac{\partial u}{\partial x}|^{\gamma_2}$:

For this monitor function, the dimensional equation for both MMPDE5 and MMPDE6 is

$$[\dot{x}] = \frac{[u]^{\gamma_2}}{[\tau][x]^{\gamma_2 - 1}} = \frac{1}{[\tau][t]^{2\gamma_2/(3p) + \gamma_2/3 - 1/3}}. \tag{24}$$

For (20) to be satisfied, we require

$$[\tau] \leq [t]^{1-2\gamma_2/(3p) - \gamma_2/3} = [u]^{(1+p/2)\gamma_2 - 3p/2}.$$

This suggests us to choose τ as

$$\tau(t) = \kappa \Big[\max_x \big| u(x,t) \big| \Big]^{(1+p/2)\gamma_2 - 3p/2 - \varepsilon}, \tag{25}$$

where ε and κ are positive constants as above.

Monitor function $M = \alpha|u|^{\gamma_1} + (1-\alpha)|\frac{\partial u}{\partial x}|^{\gamma_2}$ *with* $0 < \alpha < 1$: it is not hard to derive that, for (20) to be satisfied, τ should be chosen as

$$\tau = \kappa \min\Big(\Big[\max_x |u(x,t)|\Big]^{\gamma_1 - 3p/2 - \varepsilon}, \Big[\max_x |u(x,t)|\Big]^{(1+p/2)\gamma_2 - 3p/2 - \varepsilon}\Big) \tag{26}$$

with ε and κ positive constants as above.

In the last of this section, we shall consider the choice of time-step sizes in the simulation of blow-up solutions. We take the time steps of the form

$$\Delta t_n = \frac{\nu}{[\max_x u(x, t_{n-1})]^{\gamma}}, \tag{27}$$

where ν is a small positive constant. From (2) we know that $\max_x u(x,t_n)$ is proportional to $(T-t_n)^{-2/(3p)}$, *i.e.*,

$$\max_x u(x,t_n) \sim (T-t_n)^{-2/(3p)}.$$

Now we estimate that

$$\begin{aligned}
&\max_x u(x,t_n) - \max_x u(x,t_{n-1}) \\
&\quad \sim (T - t_{n-1} - \Delta t_n)^{-2/(3p)} - (T-t_{n-1})^{-2/(3p)} \\
&\quad = (T-t_{n-1})^{-2/(3p)}\big[\big(1-(T-t_n)^{2\gamma/(3p)-1}\nu\big)^{-2/(3p)} - 1\big] \\
&\quad \approx (T-t_{n-1})^{-2/(3p)}\left[\frac{2}{3p}(T-t_n)^{2\gamma/(3p)-1}\nu\right] \\
&\quad = \frac{2}{3p}(T-t_n)^{2\gamma/(3p)-2/(3p)-1}\nu.
\end{aligned} \tag{28}$$

To resolve the dramatic increase in the blow-up solution, we choose

$$\gamma = 1 + 3p/2(1+\varepsilon), \tag{29}$$

where ε is a small positive parameter. The increase in the blow-up solution is then

$$\max_x u(x,t_n) - \max_x u(x,t_{n-1}) = O\big((T-t_n)^{\varepsilon}\nu\big).$$

4 An analysis

In this section, we carry out a careful analysis to verify the validity of MMPDE5 in simulating blow-up solutions when the monitor function M, τ are chosen as in {(16), (26)}, respectively. Similar analysis can be performed for MMPDE5 with the choice of M, τ as in {(14), (23)} or as in {(15), (25)}. The analysis can also be conducted for MMPDE6 with the choices of M, τ above mentioned.

Now we consider (1) in the blow-up region, that is, time t is close to the blow-up time T. Write

$$x(\xi, t) = x^* + c(T-t)^{1/3} + z(\xi)(T-t)^{1/3}, \tag{30}$$

where $z(\xi)$ is a smooth function. For simplification, by differentiating (30), we obtain

$$\dot{x} = \frac{c}{3}(T-t)^{-2/3} + \frac{1}{3}(T-t)^{-2/3}z, \tag{31}$$

$$x_\xi = (T-t)^{1/3}z_\xi, \tag{32}$$

$$x_{\xi\xi} = (T-t)^{1/3}z_{\xi\xi}. \tag{33}$$

The exact form (2) gives

$$u = (T-t)^{-2/(3p)}\psi(z) + \text{bounded term}. \tag{34}$$

Hereafter we only consider the blow-up solution u while omitting the bounded term. Thus we have

$$\frac{\partial u}{\partial x} = (T-t)^{-(2+p)/(3p)}\psi'(z). \tag{35}$$

Inserting the above expressions into the monitor function (16) leads to

$$M = \alpha(T-t)^{-2\gamma_1/(3p)}\left|\psi(z)\right|^{\gamma_1} + (1-\alpha)(T-t)^{-(2+p)\gamma_2/(3p)}\left|\psi'(z)\right|^{\gamma_2},$$

$$M_\xi = \alpha(T-t)^{-2\gamma_1/(3p)}\frac{d(|\psi(z)|^{\gamma_1})}{dz}z_\xi + (1-\alpha)(T-t)^{-(2+p)\gamma_2/(3p)}\frac{d(|\psi'(z)|^{\gamma_2})}{dz}z_\xi.$$

Putting the above results into

$$\tau\dot{x} = M\frac{\partial^2 x}{\partial\xi^2} + \frac{\partial M}{\partial\xi}\frac{\partial x}{\partial\xi}, \tag{36}$$

which is an equivalent form of MMPDE5 (5), gives

$$\begin{aligned}
&\tau\left[\frac{c}{3}(T-t)^{-2/3} + \frac{1}{3}(T-t)^{-2/3}z\right] \\
&\quad = \left[\alpha(T-t)^{-2\gamma_1/(3p)+1/3}\left|\psi(z)\right|^{\gamma_1} + (1-\alpha)(T-t)^{-(2+p)\gamma_2/(3p)+1/3}\left|\psi'(z)\right|^{\gamma_2}\right]z_{\xi\xi} \\
&\qquad + \left[\alpha(T-t)^{-2\gamma_1/(3p)+1/3}\frac{d(|\psi(z)|^{\gamma_1})}{dz}\right. \\
&\qquad \left. + (1-\alpha)(T-t)^{-(2+p)\gamma_2/(3p)+1/3}\frac{d(|\psi'(z)|^{\gamma_2})}{dz}\right]z_\xi^2.
\end{aligned} \tag{37}$$

Consider the case that

$$\gamma_1 > \frac{2+p}{2}\gamma_2.$$

Let $\delta = 2\gamma_1/(3p) - (2+p)\gamma_2/(3p)$. Multiplying equation (37) with $(T-t)^{2\gamma_1/(3p)-1/3}$ gives

$$\begin{aligned}
&\tau\left[\frac{c}{3}(T-t)^{2\gamma_1/(3p)-1} + \frac{1}{3}(T-t)^{2\gamma_1/(3p)-1}z\right] \\
&\quad = \alpha\left[z_{\xi\xi}\left|\psi(z)\right|^{\gamma_1} + z_\xi^2\frac{d(|\psi(z)|^{\gamma_1})}{dz}\right] \\
&\qquad + (1-\alpha)(T-t)^{\delta}\left[z_{\xi\xi}\left|\psi'(z)\right|^{\gamma_2} + z_\xi^2\frac{d(|\psi'(z)|^{\gamma_2})}{dz}\right].
\end{aligned} \tag{38}$$

Note that in the blow-up region, z, $\frac{d(|\psi(z)|^{\gamma_2})}{dz}$, $\frac{d(|\psi'(z)|^{\gamma_2})}{dz}$ are bounded. Combining with (26) and (34), it is not hard to see the term in the left-hand side of (38) is equal to $\kappa O((T-t)^{\varepsilon})$. By omitting the term on the left-hand side and the second term on the right-hand side in (38), we obtain an ODE such that the function z approximately satisfies

$$\frac{d^2z}{d\xi^2} = -\frac{1}{|\psi(z)|^{\gamma_1}} \frac{d(|\psi(z)|^{\gamma_1})}{dz} \left(\frac{dz}{d\xi}\right)^2. \tag{39}$$

Similarly, in the case that

$$\gamma_1 < \frac{2+p}{2}\gamma_2,$$

the function z approximately satisfies

$$\frac{d^2z}{d\xi^2} = -\frac{1}{|\psi'(z)|^{\gamma_2}} \frac{d(|\psi'(z)|^{\gamma_2})}{dz} \left(\frac{dz}{d\xi}\right)^2. \tag{40}$$

For the critical case

$$\gamma_1 = \frac{2+p}{2}\gamma_2,$$

the function z approximately satisfies

$$\begin{aligned} &\left[\alpha\left|\psi(z)\right|^{\gamma_1} + (1-\alpha)\left|\psi'(z)\right|^{\gamma_2}\right]\frac{d^2z}{d\xi^2} \\ &\quad = -\left[\alpha\frac{d(|\psi(z)|^{\gamma_1})}{dz} + (1-\alpha)\frac{d(|\psi'(z)|^{\gamma_2})}{dz}\right]\left(\frac{dz}{d\xi}\right)^2. \end{aligned} \tag{41}$$

Now we determine the boundary conditions for (39), (40), (41). Since the boundary points are kept to be fixed in the mesh movement (7), we know from (30) that

$$z(0) = \left[x_L - x^* - c(T-t)^{1/3}\right](T-t)^{-1/3}; \tag{42}$$

$$z(1) = \left[x_R - x^* - c(T-t)^{1/3}\right](T-t)^{-1/3}. \tag{43}$$

To solve the boundary value problems {(39), (42), (43)}, we rewrite the ODE (39) into the form

$$\frac{d(\frac{dz}{d\xi})}{\frac{dz}{d\xi}} = -\frac{d(|\psi(z)|^{\gamma_1})}{|\psi(z)|^{\gamma_1}}.$$

Integrating this equation gives

$$\frac{dz}{d\xi} = C\left|\psi(z)\right|^{-\gamma_1},$$

or

$$\frac{d\xi}{dz} = C^{-1}\left|\psi(z)\right|^{\gamma_1},$$

regarding z as the independent variable.

Using the boundary condition (42) and (43), we obtain the solution to {(39), (42), (43)}

$$\xi = \frac{\int_{z(0)}^{z} |\psi(s)|^{\gamma_1} ds}{\int_{z(0)}^{z(1)} |\psi(s)|^{\gamma_1} ds}. \tag{44}$$

Analogously, the solutions to {(40), (42), (43)}, and {(41), (42), (43)} are given by, respectively,

$$\xi = \frac{\int_{z(0)}^{z} |\psi'(s)|^{\gamma_2} ds}{\int_{z(0)}^{z(1)} |\psi'(s)|^{\gamma_2} ds} \tag{45}$$

and

$$\xi = \frac{\int_{z(0)}^{z} [\alpha|\psi(s)|^{\gamma_1} + (1-\alpha)|\psi'(s)|^{\gamma_2}] ds}{\int_{z(0)}^{z(1)} [\alpha|\psi(s)|^{\gamma_1} + (1-\alpha)|\psi'(s)|^{\gamma_2}] ds}. \tag{46}$$

Equations (44), (45), and (46) indicate that the meshes generated by MMPDE5 in physical space can equidistribute the correspondent monitor functions M if the uniform grids are taken in ξ space. A similar analysis can be done for other choices of parameters in MMPDE5 and MMPDE6. This shows the feasibility of determining the parameters in MMPDE5 and MMPDE6 by criterion (4).

5 Numerical examples

In this section, we demonstrate the efficiency and accuracy of the proposed moving collocation method for solving GKdV equations. Example 5.1 is chosen to illustrate the rate of convergence while Examples 5.2 and 5.3 show the capability of our method to accurately capture the two important features of the GKdV equations - solitary waves and blow-up.

The moving collocation method is carried out by solving the coupled system consisting of an MMPDE and {(12), (13)}. We here use MMPDE6 in the coupled system for our numerical experiments and denote $U(x, t_n)$ the approximate solution obtained at t_n. The coupled system at t_n is solved in an alternating way. To be specific, we choose the monitor function and the temporal smoothing parameter as follows:

$$M = g_1(u, x, t), \qquad \tau = g_2(u, t).$$

We shall first solve MMPDE6 to generate the spatial mesh at t_n with

$$M(x, t_n) = g_1\big(U(x, t_{n-1}), x, t\big), \qquad \tau(t_n) = g_2\big(U(x, t_{n-1}), t\big)$$

and then solve {(12), (13)} on this mesh to obtain $U(x, t_n)$.

We mention here that the numerical solution of MMPDE6 is approximated by using central difference method for the spatial derivatives and backward Euler method for the time derivative.

One key issue in using moving mesh methods is to choose the monitor function. In order to ensure the generation of a smooth, hence more reliable, moving mesh, we add

correction terms in the choice of monitor functions. For instance, when simulating the blow-up profiles in Examples 5.2 and 5.3, we choose the monitor function as

$$M = 0.5|u| + 0.5|u_x| + \left((x-0)^2 + 0.001\right)^{-1/4} + \left((x-1)^2 + 0.001\right)^{-1/4} + C, \tag{47}$$

where the constant C is used to ensure that enough mesh points are distributed away from the blow-up region. We take $C = 2$ in our test. The third and the fourth terms are added to guarantee that enough mesh points are distributed around the end points while the first two terms capture the moving blow-up profiles. Based on the choice of monitor functions, we take τ as in (26)

$$\tau = \frac{\kappa}{(\max_x u(x,t))^{3p/2+\varepsilon-\gamma_1}},$$

with $\gamma_1 = 1$, ε being taken as 0.2 in our test. The time-step size is taken as in (29)

$$\Delta t_n = \frac{\nu}{(\max_x u(x,t_{n-1}))^{\gamma}}$$

with $\gamma = \frac{3p}{2} + 1$.

5.1 Convergence rates

We calculate the following example to show the convergence rates of the conservative collocation methods based on fixed and moving meshes.

Example 5.1 Consider the GKdV equation (1) on the space interval $[0,1]$ and on the time interval $[0,1]$ with the following initial condition:

$$u(x,0) = A\,\mathrm{sech}^{2/p}\left[K\left(x - x^0\right)\right], \tag{48}$$

where

$$K = p\left[A^p/2\epsilon(p+1)(p+2)\right]^{1/2}.$$

Then the GKdV equation (1) has the exact solution

$$u(x,t) = A\,\mathrm{sech}^{2/p}\left[K\left(x - x^0\right) - \omega t\right], \tag{49}$$

where

$$\omega = 2KA^p/(p+1)(p+2).$$

In this experiment, the time stepsize is taken to be $\Delta t = 2.5 \times 10^{-5}$. We shall vary the number of mesh subintervals N to test the order of convergence of our moving collocation method. Both cases, with a uniform mesh and with a moving mesh, are tested. The monitor function is taken as

$$M = 0.5|u| + 0.5|u_x| + 2,$$

Table 1 Results for the uniform mesh in Example 5.1

N	40	70	100	130	160
Error	1.18e–3	1.44e–4	3.56e–5	1.24e–5	5.19e–6
Rate	-	3.75	3.92	4.03	4.19

Table 2 Results for the moving mesh in Example 5.1

N	40	70	100	130	160
Error	1.02e–4	1.34e–5	3.30e–6	1.04e–6	4.06e–7
Rate	-	3.63	3.94	4.37	4.57

where applicable. For $p = 1$, $A = 2$, $\epsilon = 5 \times 10^{-4}$, $x_0 = 0.5$, the results are shown in Tables 1 and 2. In the tables, the rate of convergence is given by

$$\text{Rate} = \frac{\log(\frac{\|E_{N_1}\|_\infty}{\|E_{N_2}\|_\infty})}{\log(\frac{1/N_1}{1/N_2})}.$$

From Tables 1 and 2, we may see that the convergence rates for the conservative collocation methods are 4. The convergence order of the moving collocation method with fifth-order Hermite polynomial basis is expected to be 6; however, this is only true for some special types of PDE. For the KdV equations which are nonlinear, it is indeed not guaranteed that the moving collocation scheme can attain the sixth-order convergence. The numerical tests show that the conservative collocation methods are of high-order schemes for both fixed (uniform) meshes and moving meshes. Moreover, the error for the moving mesh is smaller than that for fixed (uniform) mesh. In fact, in the literature only one paper by Ma *et al.* [12] analyzes the convergence order of moving collocation method for linear second-order PDEs - a very simple PDE; however, it is not possible to prove the convergence rates for nonlinear KdV equations.

5.2 Capture of solitary waves and blow-up

In this section we use two examples to show the capability of our method to accurately capture the two important features of the GKdV equations - solitary waves and blow-up.

Example 5.2 For $p = 5, 6$, we consider the GKdV equation (1) on the space interval $[0, 1]$ with a small perturbation to the initial condition (48):

$$u_0 = \lambda A \operatorname{sech}^{2/p}\left[K\left(x - x^0\right)\right], \tag{50}$$

where λ is the perturbation parameter. In our tests, we take $\lambda = 1.01$, $A = 2$, $\epsilon = 5 \times 10^{-4}$, and $x_0 = 0.5$.

In these tests, the number of mesh subintervals is $N = 100$, $\kappa = 0.1(\max_x u_0(x))^{\frac{3p}{2}+0.2-1}$, and $\nu = 0.000025$ for $p = 5$, $\nu = 0.00005$ for $p = 6$ separately. The numerical results for $p = 5$ are shown in Figures 1 and 2. The six graphs of u on the physical space in Figure 2 correspond to the six curves in the right part of Figure 1. The numerical results for $p = 6$ are shown in Figures 3 and 4. The six graphs of u on the physical space in Figure 4 correspond to the six curves in the right part of Figure 3.

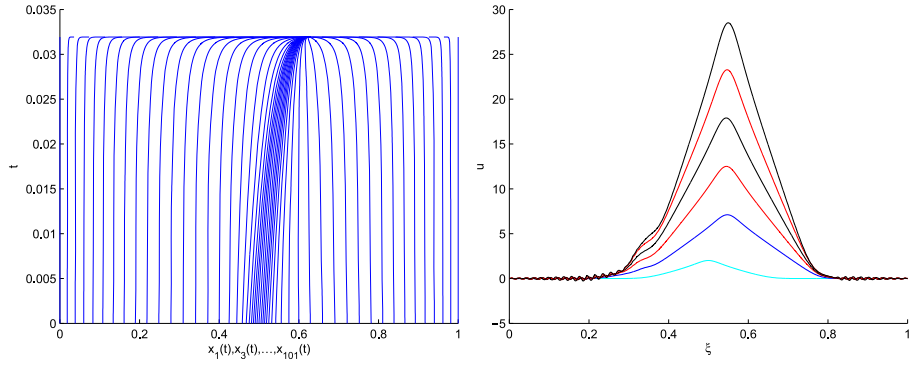

Figure 1 For $p = 5$ in Example 5.2. The left is the moving mesh $x(\xi, t)$ and the right is the blow-up profiles in the computational variable ξ.

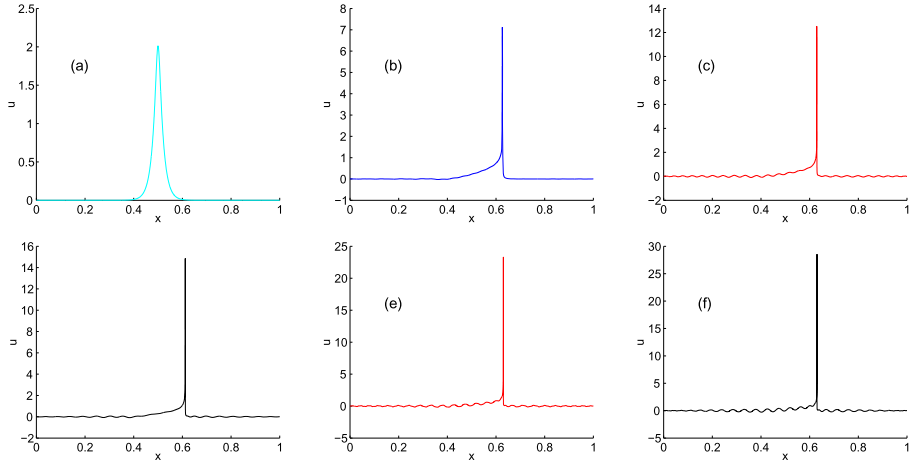

Figure 2 The blow-up profiles for $p = 5$ in Example 5.2. (a) $t = 0$, $u_{\max} = 2.02$; **(b)** $t = 2.249070196709 \times 10^{-2}$, $u_{\max} = 6.249$; **(c)** $t = 2.249391515276 \times 10^{-2}$, $u_{\max} = 10.58$; **(d)** $t = 2.249397460425 \times 10^{-2}$, $u_{\max} = 14.83$; **(e)** $t = 2.249397897417 \times 10^{-2}$, $u_{\max} = 19.13$; **(f)** $t = 2.249397956808 \times 10^{-2}$, $u_{\max} = 23.40$.

Example 5.3 When $p = 4$, we investigate the GKdV equation (1) on the space interval $[0, 1]$ with the initial profile

$$u_0 = 3e^{-100(x-0.5)^2} - 1. \tag{51}$$

In the test we take $\epsilon = 0.121 \times 10^{-3}$. The numerical results are shown in Figures 5, 6, in which the parameters N, κ are chosen as in Example 5.2 and $\nu = 0.00025$. The six graphs of u on the physical space in Figure 6 correspond to the six curves in the right part of Figure 5.

From the above tests, we can observe that the solitary waves move from one side to the other with the peak value increasingly and eventually ends up with a blow-up. Also we observe that there are oscillations in the non-blow-up regions. That means that there are also waves of small amplitude in the non-blow-up regions.

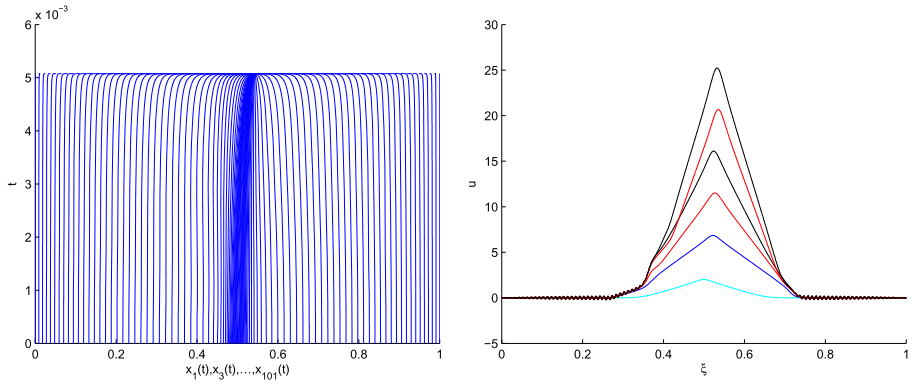

Figure 3 For $p = 6$ in Example 5.2. The left is the moving mesh $x(\xi, t)$, the right $u(\xi, t)$.

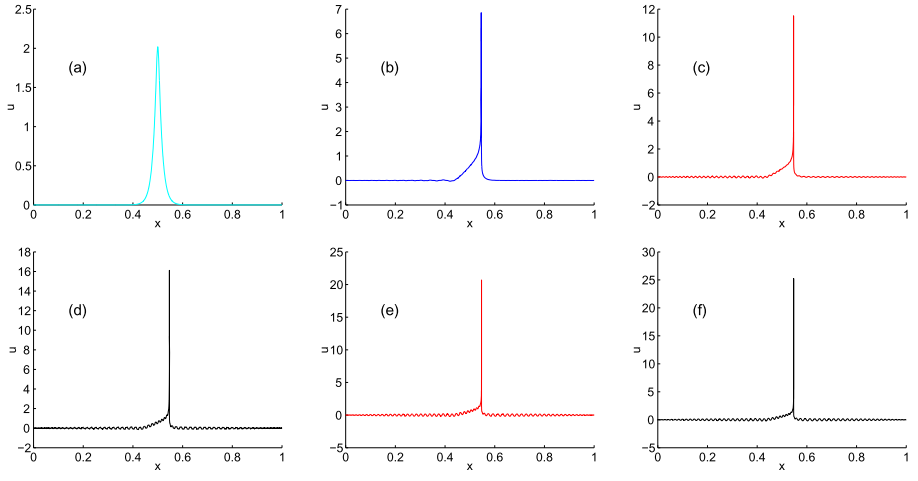

Figure 4 The blow-up profiles for $p = 6$ in Example 5.2. **(a)** $t = 0$, $u_{\max} = 2.02$; **(b)** $t = 5.077843981799 \times 10^{-3}$, $u_{\max} = 6.31$; **(c)** $t = 5.077977135290 \times 10^{-3}$, $u_{\max} = 10.43$; **(d)** $t = 5.077978558534 \times 10^{-3}$, $u_{\max} = 14.43$; **(e)** $t = 5.077978631256 \times 10^{-3}$, $u_{\max} = 18.40$; **(f)** $t = 5.077978638853 \times 10^{-3}$, $u_{\max} = 22.33$.

6 Conclusions

Applied to second- and fourth-order PDEs [9, 10], moving collocation methods show a high order of convergence and capabilities of capturing blow-up phenomena. In this paper, we develop the moving collocation method for third-order PDEs - the KdV equations. The method can be easily generalized to third-order PDEs of other types. The fully discrete moving collocation method proposed is shown to be fourth-order convergent in space and it is then employed to simulate the blow-up solutions to the generalized KdV equations. In the simulation of the blow-up solutions, we use MMPDEs to generate the moving meshes: we first assess how fast the mesh trajectory speed is required to be according to the structure of the blow-up solutions, and then determine the parameters in the MMPDEs through dimensional analysis. The theoretical analysis and the numerical experiments show that the method can accurately capture the two important features of the GKdV equation - solitary waves and blow-up.

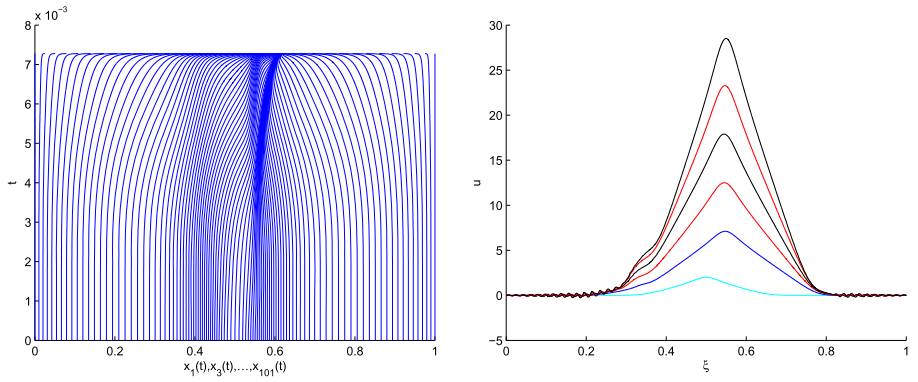

Figure 5 For $p = 4$. The left is moving mesh $x(\xi, t)$, the right $u(\xi, t)$.

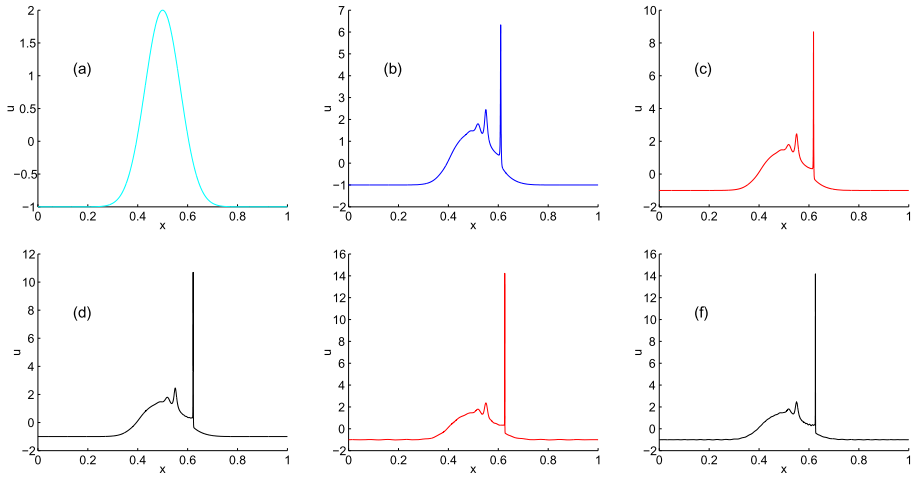

Figure 6 The blow-up profiles for $p = 4$ in Example 5.3. (a) $t = 0$, $u_{\max} = 2$; **(b)** $t = 7.245823777296 \times 10^{-3}$, $u_{\max} = 6.989$; **(c)** $t = 7.273839836925 \times 10^{-3}$, $u_{\max} = 9.756$; **(d)** $t = 7.277618404530 \times 10^{-3}$, $u_{\max} = 12.12$; **(e)** $t = 7.278608365592 \times 10^{-3}$, $u_{\max} = 14.22$; **(f)** $t = 7.278965443315 \times 10^{-3}$, $u_{\max} = 16.12$.

Competing interests
The authors declare that they have no competing interests.

Authors' contributions
XW carried out the analysis in Section 4 and ZZ made the main contributions to the other sections. All authors read and approved the final manuscript.

Acknowledgements
The authors are grateful to Prof. J Ma for the helpful suggestions.

Received: 1 November 2015 Accepted: 26 January 2016 Published online: 18 February 2016

References

1. Korteweg, DJ, de Vries, G: On the change of form of long waves advancing in rectangular canal and on a new type of long stationary wave. Philos. Mag. **39**, 422-443 (1895)
2. Miura, RM: A remarkable explicit nonlinear transformation. J. Math. Phys. **9**, 1202-1205 (1968)
3. Bona, JL, Souganidis, PE, Strauss, WA: Stability and instability of solitary waves of KdV type. Proc. R. Soc. Lond. A **411**, 395-412 (1987)
4. Bona, JL, Weissler, FB: Similarity solutions of the generalized Korteweg-de Vries equation. Math. Proc. Camb. Philos. Soc. **127**, 323-351 (1999)
5. Bona, JL, Dougalis, VA, Karakashian, OA, McKinney, WR: Conservative, high-order numerical schemes for the generalized Korteweg-de Vries equation. Philos. Trans. R. Soc. Lond. A **351**, 107-164 (1995)
6. Bona, JL, Dougalis, VA, Karakashian, OA, McKinney, WR: The effect of dissipation on solutions of the generalized Korteweg-de Vries equation. J. Comput. Appl. Math. **74**, 127-154 (1996)

7. Budd, CJ, Huang, WZ, Russell, RD: Moving mesh methods for problems with blow-up. SIAM J. Sci. Comput. **17**, 305-327 (1996)
8. Huang, WZ, Ren, Y, Russell, RD: Moving mesh partial differential equations (MMPDEs) based upon the equidistribution principle. SIAM J. Numer. Anal. **31**, 709-730 (1994)
9. Huang, WZ, Russell, RD: A moving collocation method for the numerical solution of time dependent differential equations. Appl. Numer. Math. **20**, 101-116 (1996)
10. Russell, RD, Williams, JF, Xu, X: MOVCOL4: a moving mesh code for fourth-order time-dependent partial differential equations. SIAM J. Sci. Comput. **29**, 197-220 (2007)
11. Ma, J, Jiang, Y: Moving collocation methods for time fractional differential equations and simulation of blowup. Sci. China Math. **54**, 611-622 (2011)
12. Ma, J, Huang, WZ, Russell, RD: Analysis of a moving collocation method for one-dimensional partial differential equations. Sci. China Math. **55**, 827-840 (2012)
13. Huang, WZ, Ma, J, Russell, RD: A study of moving mesh PDE methods for numerical simulation of blowup in reaction diffusion equations. J. Comput. Phys. **227**, 6532-6552 (2008)
14. Huang, WZ, Russell, RD: A moving collocation method for the numerical solution of time dependent differential equations. Appl. Numer. Math. **20**, 101-116 (1996)